Supporting Information

Zinc Pyrovanadate Nanoplates Embedded in Graphene Networks with Enhanced Electrochemical Performance

Yang Yu,[†,#] Chaojiang Niu,[†,#] Chunhua Han,*[,†] Kangning Zhao,[†] Jiashen Meng,[†] Xiaoming Xu,[†] Pengfei Zhang,[†,‡] Lei Wang,[†] Yuzhu Wu,[†] and Liqiang Mai*[,†]

[†]State Key Laboratory of Advanced Technology for Materials Synthesis and Processing, Wuhan University of Technology, Wuhan 430070, Hubei, China.

[‡]Department of Chemistry, Shanghai Key Laboratory of Molecular Catalysis and Innovative Materials, Laboratory of Advanced Materials, Fudan University, Shanghai, 200433, China

Corresponding Author

*E-mail: mlq518@whut.edu.cn.

*E-mail: hch5927@gmail.com.

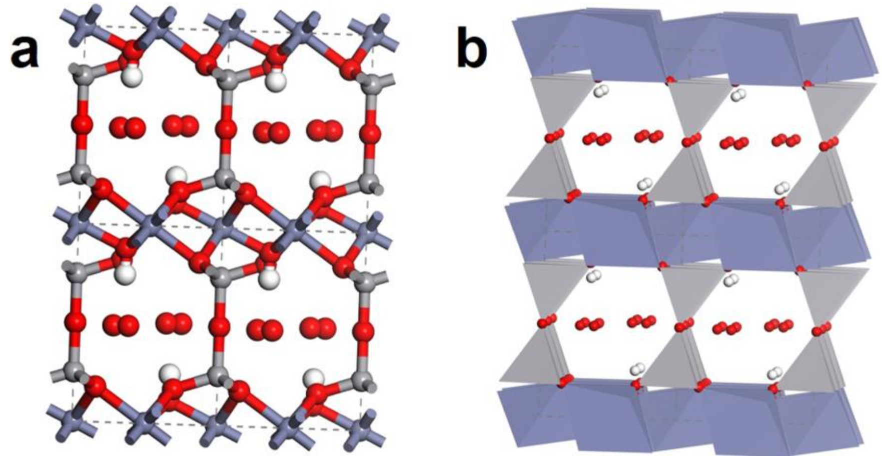

Figure S1. Crystal structure of $Zn_3V_2O_7(OH)_2{\cdot}2H_2O$ phase, (a) ball-and-stick model, (b) polyhedral model.

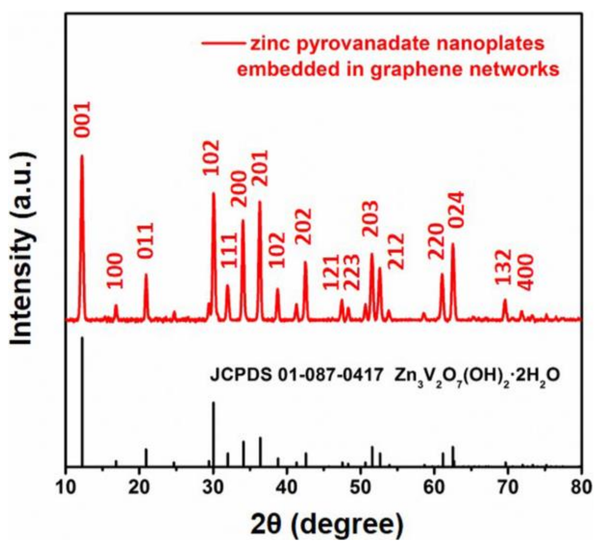

Figure S2. XRD pattern of zinc pyrovanadate nanoplates embedded in graphene networks.

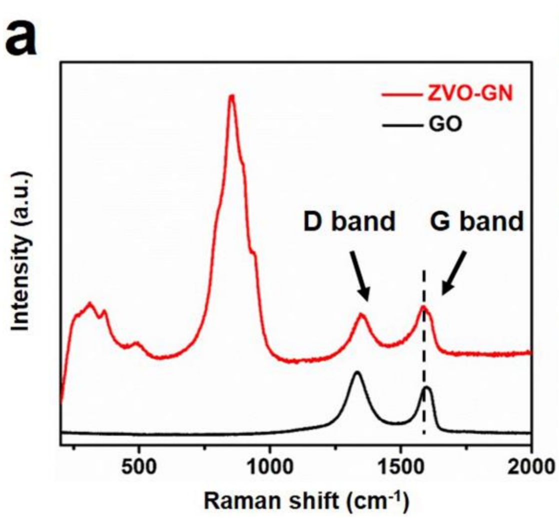

Figure S3. (a) Raman spectra and (b) TGA curves of zinc pyrovanadate nanoplates and zinc pyrovanadate nanoplates embedded in graphene networks, respectively.

Table S1. The results of C, H, N, S element analysis of two samples of zinc pyrovanadate nanoplates embedded in graphene networks.

Sample mass (mg)	N (%)	C (%)	H (%)	S (%)
5.05	**0.00**	**3.62**	**1.38**	**0.00**
5.35	**0.00**	**3.63**	**1.33**	**0.00**

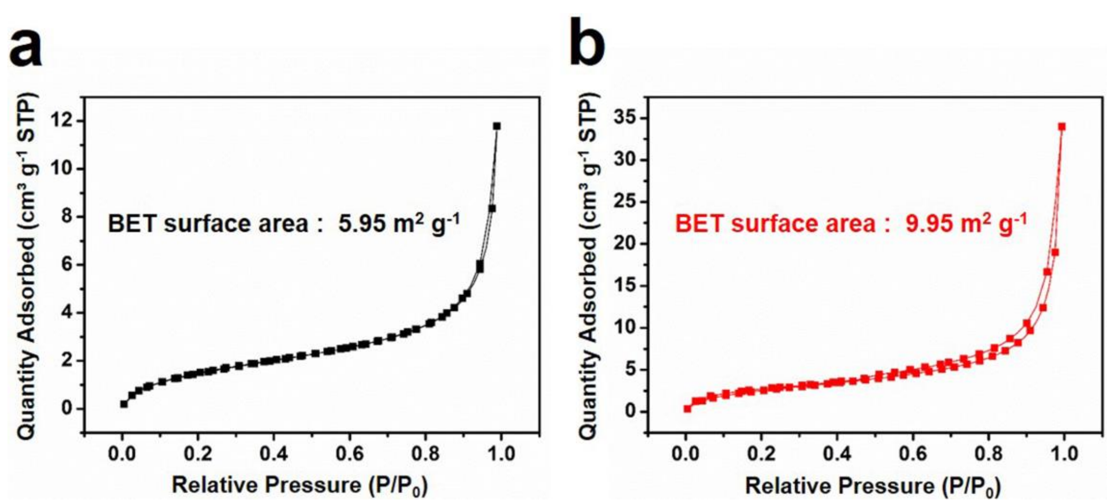

Figure S4. N_2 adsorption/desorption isotherms of zinc pyrovanadate nanoplates (a) and zinc pyrovanadate nanoplates embedded in graphene networks (b).

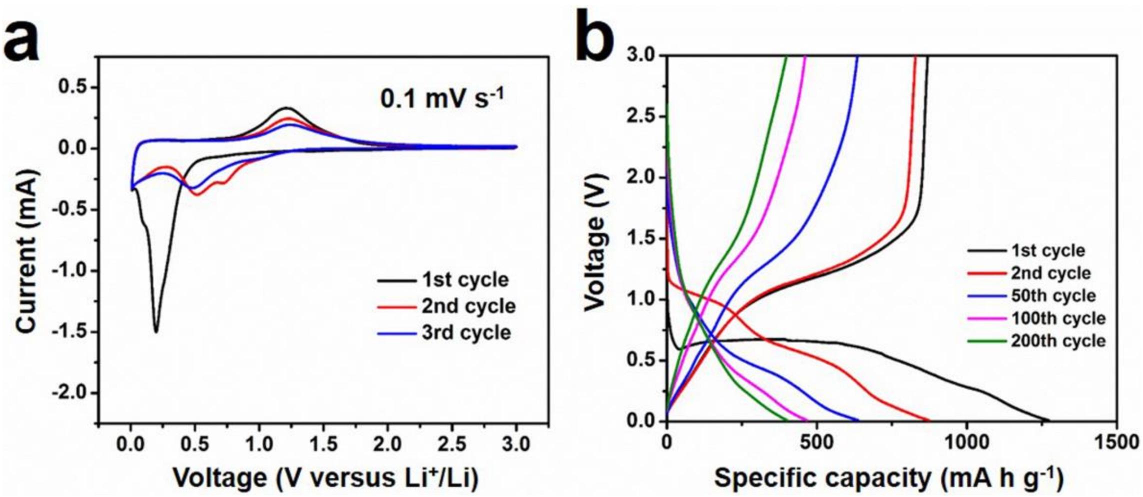

Figure S5. (a) CV curves of pristine zinc pyrovanadate nanoplates obtained at a voltage range of 0.01 to 3.0 V (vs. Li^{+}/Li) at a scan rate of 0.1 mV s^{-1}; (b) Discharge and charge profiles plotted for the 1st, 2nd, 50th, 100th and 200th cycles of pristine zinc pyrovanadate nanoplates at a current density of 200 mA g^{-1}.

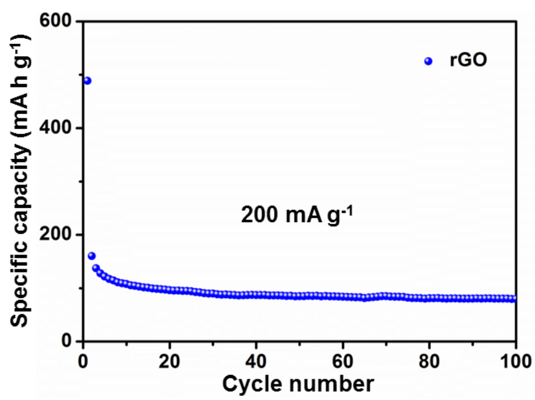

Figure S6. Cycling performance of the reduced graphene oxide after hydrothermal treatment at 180 ^{o}C for 18 h as anode for LIBs at a current density of 200 mA g^{-1}, respectively.

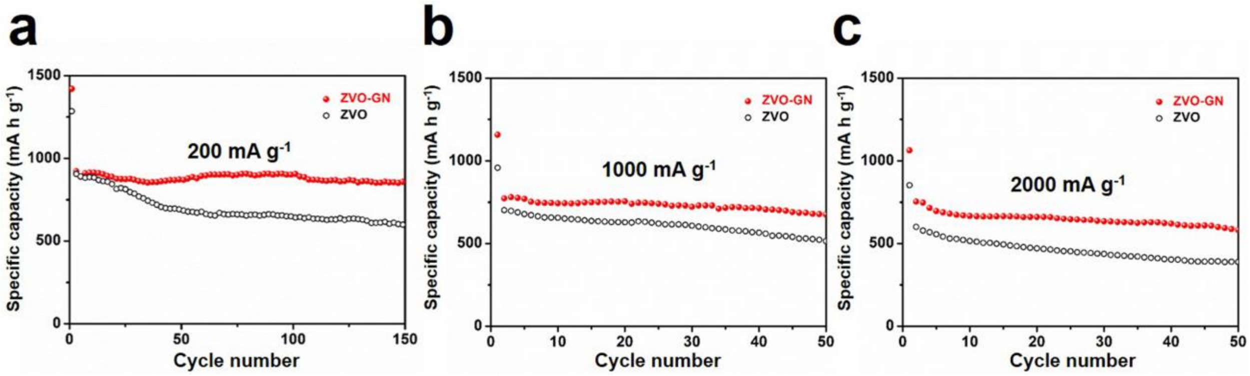

Figure S7. Cycling performance of zinc pyrovanadate nanoplates and zinc pyrovanadate nanoplates embedded in graphene networks at current density of 200 mA g^{-1}, 1000 mA g^{-1} and 2000 mA g^{-1}, respectively.

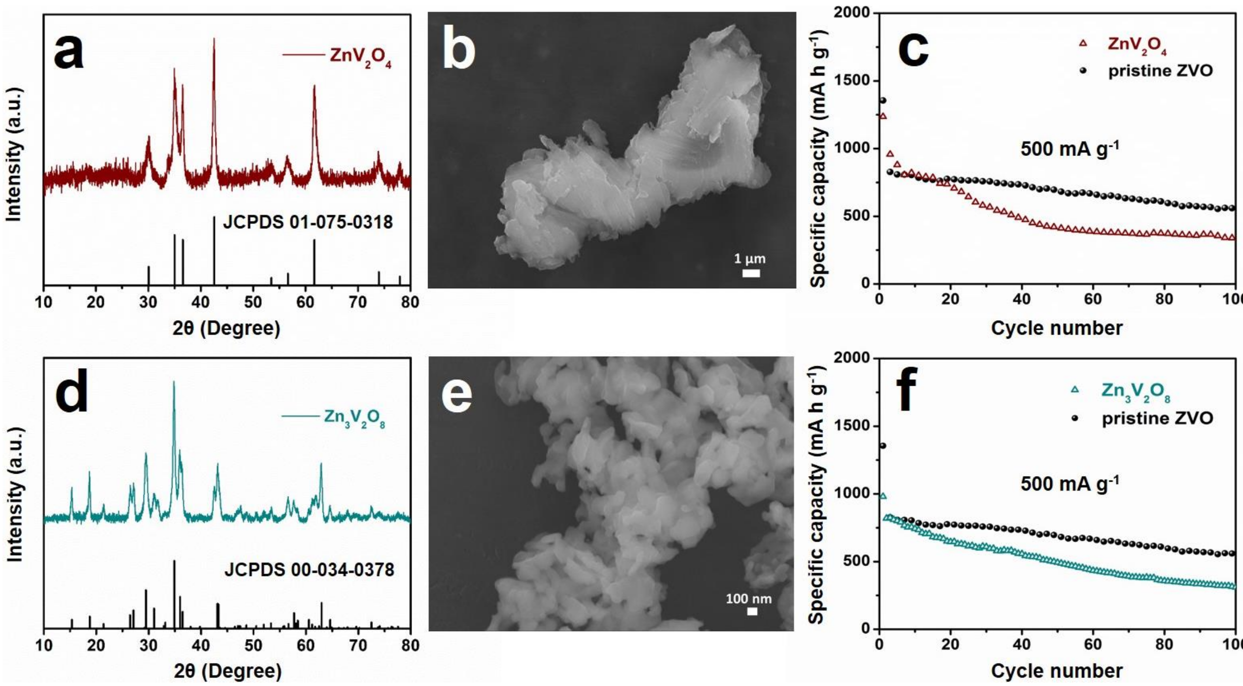

Figure S8. XRD patterns of ZnV_2O_4 (a) and $Zn_3V_2O_8$ (d). SEM images of ZnV_2O_4 (b) and $Zn_3V_2O_8$ (e). Cycling performances of ZnV_2O_4 (a) and $Zn_3V_2O_8$ (d) at the current density of 500 mA g^{-1}. The ZnV_2O_4 and $Zn_3V_2O_8$ are prepared by annealing zinc pyrovanadate nanoplates embedded in graphene networks in Ar and in air at 500 $^{\circ}$C for 4 h, respectively.

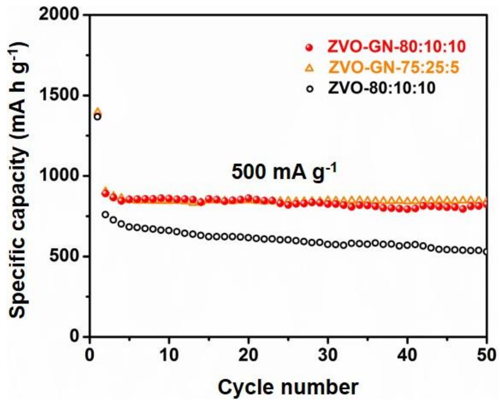

Figure S9. Electrochemical performance comparisons between the electrode consist of 80% ZVO, 10% acetylene black and 10% CMC, the electrode consist of 80% ZVO-GN, 10% acetylene black and 10% CMC and the electrode consist of 75% ZVO-GN, 25% acetylene black and 5% CMC at a current density of 500 mA g^{-1}.

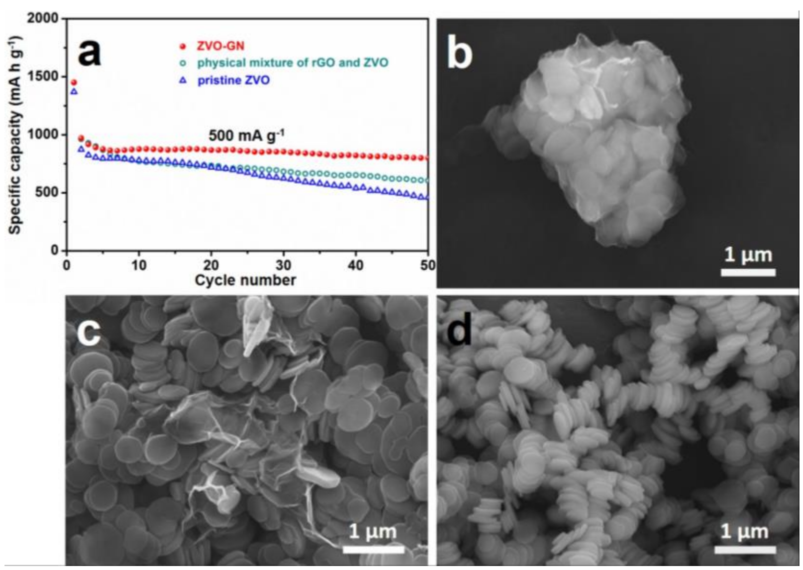

Figure S10. Cycling performances of zinc pyrovanadate nanoplates embedded in graphene networks, physical mixture of zinc pyrovanadate nanoplates and graphene oxide, and bare zinc pyrovanadate nanoplates at a current density of 500 mA g^{-1}. SEM images of (b) zinc pyrovanadate nanoplates embedded in graphene networks, (c) physical mixture of zinc pyrovanadate nanoplates and graphene oxide, and (d) bare zinc pyrovanadate nanoplates.

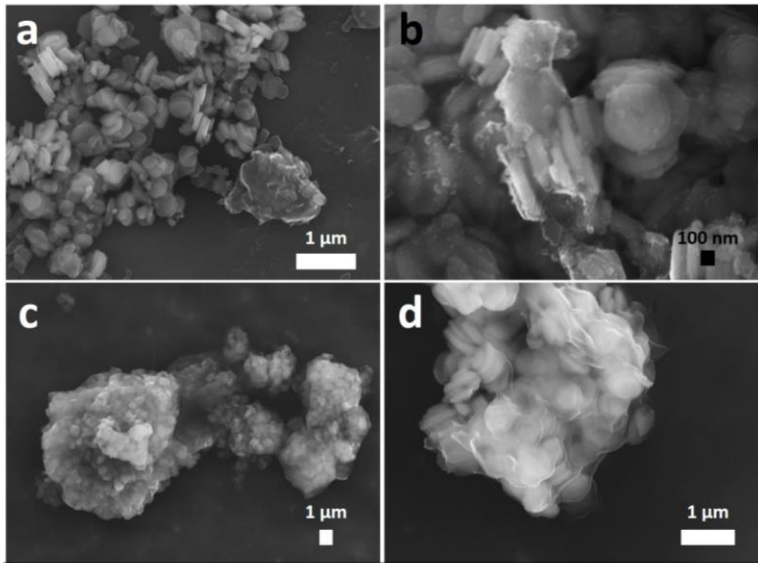

Figure S11. SEM images of zinc pyrovanadate nanoplates (a, b) and zinc pyrovanadate nanoplates embedded in graphene networks (c, d) after 50 cycles at the current density of 500 mA g^{-1}.

Table S2. Comparison of electrochemical performances between zinc pyrovanadate nanoplates and zinc pyrovanadate nanoplates embedded in graphene networks at different current densities.

Material	Current density (mA g^{-1})	Initial reversible capacity (mA h g^{-1})	Cycle number	Capacity retention (%)
ZVO-GN	200	953	150	90
	1000	773	50	88
	2000	753	50	77
ZVO	200	930	150	64
	1000	702	50	73
	2000	601	50	65

Table S3. Comparison of electrochemical performances between this work and other previous works.

Electrode	Reversible capacity (mA h g^{-1})	Current density (mA g^{-1})	Cycle number	Remained capacity (mA h g^{-1})	Voltage range (vs. Li^+/Li)
ZVO-GN (this work)	**1053** **902**	**200** **500**	**200** **400**	**930** **854**	**0.01-3.0 V**
Ultralong monoclinic ZnV_2O_6 nanowires[21]	1035	100	10	973	0.025-3.0 V
ZnV_2O_4-CMK nanocomposite[25]	424 (from 5th cycle)	100	200	575	0.02-3.0 V
Hierarchical ZnV_2O_4 microspheres[30]	603	100	280	638	0.02-3.0 V
$Zn_3V_2O_7(OH)_2\cdot 2H_2O$ nanobelts[31]	874	20	20	750	0.02-2.5 V
$Zn_3V_2O_7(OH)_2\cdot 2H_2O$ 3D microspheres[32]	802	20	20	619	0.02-2.5 V
$Zn_3V_2O_8$ 3D microspheres[32]	677	20	20	492	0.02-2.5 V